JOURNAL OF MATERIALS SCIENCE 9 (1974) 1609–1614

Impact fracture of compact bone in a shock tube

W. BONFIELD, P. K. DATTA*
Department of Materials, Queen Mary College, London, UK

A shock tube technique was utilized to assess the impact fracture of bovine femur compact bone, in the form of cylindrical tube specimens. The effect of wall thickness on the fracture pressure was established and an unique hoop stress (= 18.0 MN m^{-2}) for fracture obtained. In addition, the effect of crack length and radius of curvature of the crack tip on the fracture hoop stress was established, together with a determination of Young's modulus at the shock loading rate. The possible correlations of these results with fracture mechanics concepts are discussed.

1. Introduction

In a previous study by Bonfield and Li [1] the fracture behaviour of compact bone sections under impact loading conditions was established. The method utilized was the traditional Charpy test, in which a short beam specimen (both with and without an edge crack) was struck by a swinging hammer. It is recognized that this particular method has two disadvantages. First, as the specimen is fractured in bending, the stress field within the specimen is non-uniform. Second, an oscillatory loading pattern is produced if the stiffness of the specimen does not match that of the hammer. An alternative method of impact testing which has recently been developed by Reed and Squires [2] utilizes a shock tube to deliver an internal impulsive load to a specimen in the form of a thin walled cylinder. Hence, impact loading in this manner has the advantage that fracture of the specimen is produced under an essentially uniform hoop stress.

In this paper, the first application of a shock tube technique to assess the impact fracture of thin-walled cylinders taken from bovine femur compact bone sections is reported. The effect of wall thickness on the fracture pressure was established and an unique hoop stress for fracture obtained. In addition, the effect of crack length and radius of curvature of the crack tip on fracture strength was measured, together with a determination of Young's modulus at the shock loading rate. The possible correlation of these results with fracture mechanics concepts are discussed.

2. Experimental procedure

The general shock tube assembly and operation has been discussed in detail previously [2, 3]. It consists of a driver and driven section (i.d. 42.4 mm), a double diaphragm section and a dump tank containing the specimen clamping fixture, which acts as a pressure vessel extension of the shock tube. The cylindrical specimens are mounted to form an extension of the driven section within the dump tank. The test specimen is axially clamped between two end plates, with the clamping pressure just sufficient to prevent the specimen from falling under its own weight.

Thin walled cylindrical specimens were machined from 2 to 3 year bovine femur sections and were of length 25.4 mm, wall thickness 0.18 to 1.52 mm and i.d. 38.1 mm. The femur section was first gripped by four adjustable supports and the internal diameter obtained by slow-speed boring. The machined internal surface was then mounted on an expandable, PVC coated, mandrel and the external diameter prepared by slow-speed turning. The specimen length was less than the length of the shock pulse, i.e. the length of the travelling high pressure gas zone between the shock front and

*Present address: Department of Chemistry and Metallurgy, Glasgow College of Technology.

the following rarefaction wave, and hence the whole specimen was subjected to a uniform internal pressure during subsequent testing.

Cracks of various lengths (2.2 to 19.8 mm) and radii of curvature (0.19 to 1.23 mm) were produced in the walls of the tubular specimen by drilling through the wall at one end of the required crack and then traversing the drill along a generator of the cylinder. During machining and up to the time of test, the specimen was kept in Ringer's solution. A typical test specimen is shown in Fig. 1.

Figure 1 A cylindrical tube bovine femur compact bone specimen (of length 25.4 mm), containing a longitudinal crack of length, $2c$, = 2.2 mm, fractured under internal shock loading. (Note — the fractured specimen has been secured with a section of tape which can be seen in the figure.)

To perform an impact test, the pressures of the driven and driven gases, nitrogen and air respectively, were adjusted to generate a shock pulse of the required magnitude. Each specimen was subjected to a series of shock pulses of increasing pressure until fracture occurred. In addition, the strain produced by each shock pulse was measured by the strain gauge technique previously reported by Bonfield and Clark [4].

The shock pressure, P_2, was calculated from measurements of the driver gas pressure, P_4, and driven gas pressure, P_1, using the relationships:

$$\frac{P_4}{P_1} = \frac{2\gamma_1 M^2 - (\gamma_1 - 1)}{(\gamma_1 + 1)} \left\{1 - \frac{(\gamma_4 - 1)}{(\gamma_1 + 1)} \frac{a_1}{a_4}\left(M - \frac{1}{M}\right)\right\}^{-2\gamma_4/\gamma_4 - 1} \quad (1)$$

$$\frac{P_2}{P_1} = \frac{2\gamma_1 M^2 - (\gamma_1 - 1)}{\gamma_1 + 1} \quad (2)$$

where γ_1 and γ_4 are the ratio of specific heats of the driven and driver gas respectively, a_1 and a_4 are the velocity of sound in the driven and driver gas respectively, and M is the shock Mach number. The shock pulse pressure was then converted to the hoop stress, by the expression

$$\sigma_\theta = P_2 R/t \quad (3)$$

where R and t are the radius and wall thickness of the specimen. This expression for hoop stress is derived from equilibrium considerations of a statically loaded thin walled cylinder subjected to an internal pressure, P_2. It is considered by Reed and Squires [2] that this expression is applicable to impulse loading and its general form is verified experimentally in the present study.

3. Experimental results

3.1. Effect of wall thickness on the pressure for fracture

A series of cylindrical tube specimens were prepared, with a constant length (25.4 mm) and internal radius, R (19.1 mm), but with a series of wall thicknesses, t, ranging from 0.18 to 1.52 mm. For each specimen the minimum shock pressure (P_2) required for fracture was measured at a loading rate of 1.8 GN m^{-2} sec^{-1}. The results obtained which are shown in Fig. 2, give a good

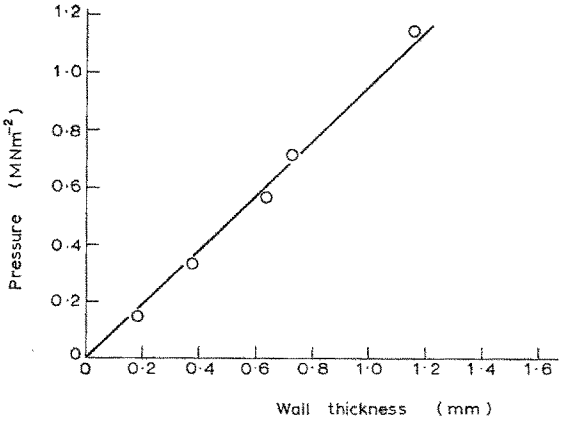

Figure 2 The effect of wall thickness on the pressure required to fracture an "uncracked" compact bone tube specimen. The full circle represents an unbroken specimen.

fit to an equation of the form

$$P_2 = kt \qquad (4)$$

where k is a constant for the range of t to 1.16 mm. The maximum pressure available was not sufficient to fracture the specimen with t = 1.52 mm (this point is shown as a full circle in Fig. 2). Hence combining Equations 3 and 4, we have that the single hoop stress (σ_θ) for fracture is given by

$$\sigma_\theta = kR$$
$$= 18.0 \text{ MN m}^{-2}.$$

As the hoop stress acts circumferentially and the fracture occurs parallel to the long axis (see Fig. 1), the fracture stress value represents the transverse fracture strength. This distinction is required in view of the anisotropy of ultrastructure (and properties) in femur compact bone.

3.2. Measurement of Young's modulus

The deformation prior to fracture of five identical cylindrical tube specimens, with wall thickness, t, = 0.38 mm, was measured for a loading rate of 1.8 GN m^{-2} sec^{-1} (or stressing rate = 90 GN m^{-2} sec^{-1}). The circumferential strains produced by an increasing series of shock pressures, P_2 (and resultant hoop stresses, σ_θ,) for the two specimens giving limiting values, are plotted in Fig. 3. It can be seen that the deformation is approximately Hookean and this result gives two values of Young's modulus, taken from the linear slopes, of 11.6 and 14.8 GN m^{-2}, respectively. As both stress and strain are produced circumferentially and, hence, act perpendicularly to the long axis of the bone, the measured elastic modulus is the transverse Young's modulus.

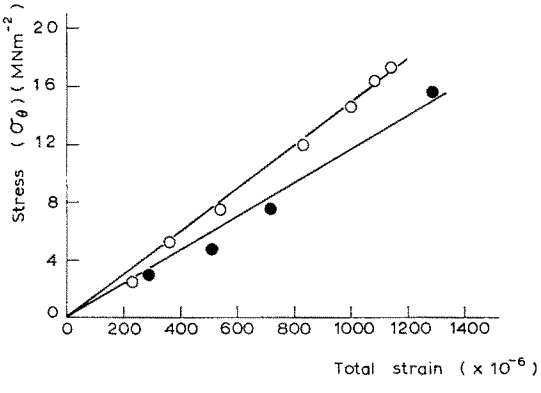

Figure 3 The variation of total strain with hoop stress for the two limiting specimens impact tested at a strain-rate of 7 sec^{-1}.

Taking an average value of Young's modulus as 13.2 GN m^{-2}, we have that the measured stressing rate of 90 GN m^{-2} sec^{-1} corresponds to a strain-rate of 7 sec^{-1}.

3.3. The effect of crack length, 2c, on the fracture stress, σ_θ

An axial crack, with a length ($2c$) ranging from 2.2 to 19.8 mm in different specimens, was machined along the long axis of a cylindrical tube specimen, with the midpoint of the crack at the midpoint of the cylinder (see Fig. 1). For each specimen the width of the crack was 0.76 mm, the radius of curvature of the crack tip, r, was 0.38 mm and the wall thickness, t, was 0.38 mm. The fracture stress, σ_θ, measured at a strain-rate of 7 sec^{-1} for various crack lengths, $2c$, is shown in Fig. 4 as a function of the semi-crack length, c. The results are plotted as bars to indicate the experimental scatter between two identical specimens. It can be seen, first, that the fracture stress values are significantly less than that of the uncracked specimens (18.0 MN m^{-2}) and, second, that the fracture stress decreases as the semi-crack length, c increases. The average fracture stress (shown as open circles) is also plotted in Fig. 4 as a function of $c^{-\frac{1}{2}}$, which, except for one point, gives a relation

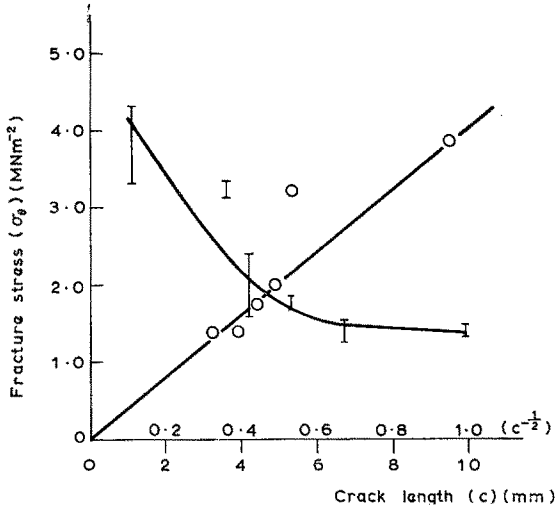

Figure 4 The variation of impact fracture stress with crack length, c, (shown as bars) and $c^{-\frac{1}{2}}$ (shown as open circles).

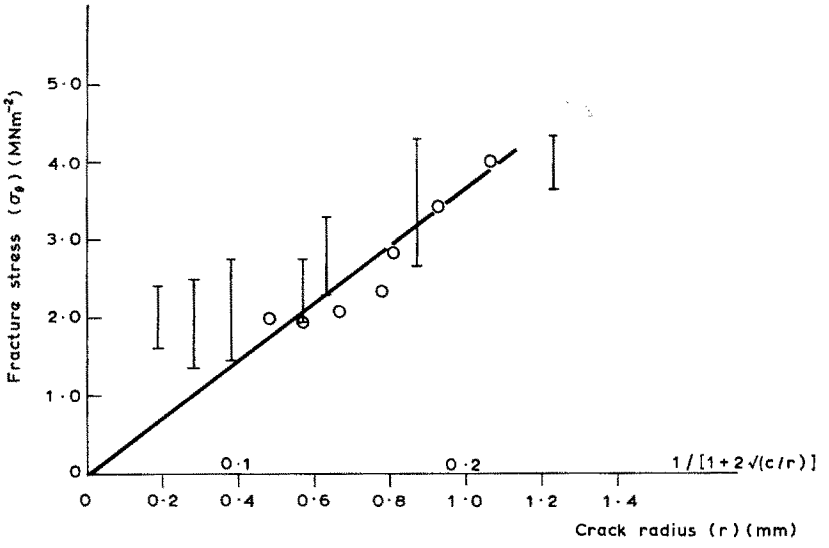

Figure 5 The variation of impact fracture stress with crack tip radius of curvature, r, (shown as bars) and $1/[1 + 2\sqrt{(c/r)}]$ (shown as open circles).

$$\sigma_\theta = Ac^{-\frac{1}{2}} \quad (5)$$

where A is a constant (= 0.13 MN m$^{-3/2}$).

3.4. The effect of crack radius of curvature, r, on the fracture stress, σ_θ

The experiments described in Section 3.3. were repeated, with a constant crack length, $2c$, of 8.4 mm, but with a crack tip radius of curvature, r, ranging from 0.19 to 1.23 mm. The fracture stresses, σ_θ, measured, at a strain-rate of 7 sec^{-1}, for the various radii of curvature, r, as plotted in Fig. 5 (as bars to represent the experimental scatter between two identical specimens). It can be seen that the fracture stress increases with an increase in the radius of curvature. Fig. 5 also reveals that the average fracture stress (shown as open circles) may be approximately fitted to an equation

$$\sigma_\theta = B \times 1/[1 + 2\sqrt{(c/r)}] \quad (6)$$

where B is a constant (= 18.5 MN m^{-2}).

4. Discussion

4.1. Impact fracture stress of uncracked specimens

The results demonstrate that there is a unique, and constant, hoop stress for impact fracture under internal pressurization, between cylindrical tube specimens with *different* dimensions. Consequently, the stress value obtained (18.0 MN m^{-2}) may be considered as an intrinsic property of compact bone under shock loading conditions. As fracture occurred parallel to the long axis of the bone and, consequently, along rather than across the collagen fibres and hydroxyapatite crystalline aggregates, then the fracture stress relates to the transverse orientation. Consequently, it is interesting to note that the impact fracture stress, with a strain-rate of 7 sec^{-1}, is smaller than the fracture stress of transversely oriented bovine femur specimens (56 MN m^{-2}) measured, in tension, at a lower strain-rate ($\sim 10^{-4}$ sec^{-1}) [5].

4.2. The transverse Young's modulus during shock loading

The transverse Young's modulus (E_t) determined during shock loading is of significance, as there is no comparable data at such a high strain-rate (7 sec^{-1}). The average measured value of 13.2 GN m^{-2} compares with the longitudinal Young's modulus (E_l) of 28 GN m^{-2} determined (in compression) at a similar high strain-rate (1 sec^{-1}) by McElhaney [6]. Consequently, the ratio between the transverse and longitudinal Young's modulus at a high strain-rate appears similar to that found originally for human femur sections by Dempster and Liddicoat [7] at a lower strain-rate ($\sim 10^{-4}$ sec^{-1}), for which $E_l \sim 2E_t$. However, this comparison may underestimate the actual ratio of E_t to E_l, as other work on the longitudinal

Young's modulus, e.g. [8], has indicated an absolute value (at 10^{-4} sec^{-1}) $\sim 50\%$ larger than that found by McElhaney [6] at approximately the same strain-rate. Consequently, if this difference is translated to the high strain-rate situation (7 sec^{-1}), we would have $E_l \sim 3.5\ E_t$. This effect will be further studied.

The transverse Young's modulus of 13.2 GN m^{-2} measured at 7 sec^{-1} compares with a value of $E_t = 9.35$ GN m^{-2} determined [5] on bovine femur specimens at a strain-rate of $\sim 10^{-4}$ sec^{-1}. Hence, although a comparison between different absolute values must be made with caution [8] it appears that the transverse Young's modulus increases with strain-rate in a similar manner to that demonstrated for the longitudinal Young's modulus [6].

4.3. The effect of crack length, 2c, and radius of curvature, r, on fracture stress

In a parallel study by Bonfield and Datta [9] the effects of edge cracks, of length c and radius of curvature r on the fracture of longitdinally oriented bovine compact bone specimens, in tension at a strain-rate of 10^{-4} sec^{-1}, were established. In contrast the present results provide data on the effect of cracks on the fracture stress of transversely oriented samples at a high strain-rate (7 sec^{-1}). The data are represented by

$$\sigma_\theta = Ac^{-\frac{1}{2}} \tag{5}$$

where A is a constant (= 0.13 MN m$^{-3/2}$).

Equation 5 compares with the following equation found for the fracture stress, σ_{fr}, for the longitudinal orientation [9]:

$$\sigma_{fr} = 2.60\, c^{-\frac{1}{2}} - 13.5\,. \tag{7}$$

In general, for a semi-infinite sheet containing a centre notch of length $2c$ (which represents the present experimental situation), we have (e.g. [10]) that the stress intensity factor, K, is given by

$$K = \sigma(\pi c)^{\frac{1}{2}}\,. \tag{8}$$

The critical stress intensity factor, K_{IC}, is given by

$$K_{IC} = \sigma_{fr}(\pi c)^{\frac{1}{2}} \tag{9}$$

where σ_{fr} is the uniaxial stress required to fracture a specimen. For an elastic solid, we also have [11] that

$$K_{IC} = (2E\gamma)^{\frac{1}{2}} \tag{10}$$

where E is Young's modulus and γ is the specific surface energy for fracture.

Substitution of the experimental results into Equations 8 to 10 yields $K_{IC} = 0.23$ MN m$^{-3/2}$ and $\gamma = 2.0$ J m^{-2}. These values are significantly less than those determined [9] for longitudinal sections (at 10^{-4} sec^{-1}), of $K_{IC} = 4.6$ MN m and $\gamma = 3.9 \times 10^2$ to 5.6×10^2 J m^{-2}. A correction associated with the "finite width" of the specimen [2] only results in a small reduction of the slope A and hence K_{IC}, and is neglected in this discussion. A potentially more significant error associated with the above derivation arises from any non-elastic deformation, prior to fracture which will produce a derived value of surface energy (γ') larger than the actual intrinsic surface energy (γ). However, the stress–strain curves (Fig. 3) indicate that non-elastic deformation is negligible for the transverse orientation, at a high strain-rate, and hence

$$\gamma'_{\text{transverse}} \sim \gamma_{\text{transverse}}\,. \tag{11}$$

In contrast, the longitudinal sections exhibit a significant level of non-elastic deformation prior to fracture and we have

$$\gamma'_{\text{longitudinal}} > \gamma_{\text{longitudinal}}\,. \tag{12}$$

Hence, the measured ratio of $\gamma'_{\text{longitudinal}}/\gamma'_{\text{transverse}}$ represents an over estimate of $\gamma_{\text{longitudinal}}/\gamma_{\text{transverse}}$.

The experimentally derived Equation 5 between σ_θ and c, may be extrapolated to the particular value of σ_θ (18.0 MN m^{-2}) obtained for a crack-free specimen and a measure of the "intrinsic crack length" c_0 obtained. This procedure gives $c_0 = 48$ μm and, hence, an internal crack length $2c_0 = 96$ μm, which approximates to the scale of the vascular spaces (20 to 100 μm). However, at this stage, the possibility that the intrinsic crack is actually an artificial crack, introduced by the specimen surface preparation, cannot be excluded.

The present results also indicate that σ_θ for fracture depends on the radius of curvature of the crack tip and can be approximately represented by the Inglis equation [10], as

$$\sigma_m = \sigma[1 + 2\sqrt{(c/r)}] \tag{13}$$

where σ_m represents the maximum stress at the crack tip, oriented perpendicularly to the tensile stress. We have then, as σ_m is equal to the constant B in Equation 6, that $\sigma_m = 18.5$ MN m^{-2}. Hence, σ_m is approximately equal to σ_θ for fracture of the uncracked specimens (= 18.0

MN m^{-2}). As this result apparently suggests that, for uncracked specimens, the critical value of c/r for fracture is $\ll 1$, it appears that the measured values of the machined radius of curvature, r, utilized in the derivation of B are considerably larger than the actual values of the radius of curvature, r_0, of the propagating crack but that r_0 does depend on r. In this context, it should be noted that the fracture stress of the longitudinal specimens [9], (which occurred at significantly higher stress levels), was independent of the crack radius of curvature. The effect of the radius of curvature on fracture stress will be studied further, with particular reference to the geometry of the vascular spaces in bovine compact bone.

5. Conclusions

1. The hoop stress, σ_θ, for fracture of a cylindrical tube bovine femur compact bone specimen in a shock tube is 18.0 MN m^{-2}.

2. The average transverse Young's modulus at a strain-rate of 7 sec^{-1} is 13.2 GN m^{-2}.

3. The hoop stress for fracture under shock loading, σ_θ, of a cylindrical tube compact bone specimen, containing an axial crack of length $2c$ is given by $\sigma_\theta = 0.13\ c^{-\frac{1}{2}}$.

4. The critical stress intensity factor (K_{IC}) is 0.23 MN $m^{-3/2}$, the specific surface energy, γ, is 2.0 J m^{-2} and the "intrinsic crack length", $2c_0$, is 96 μm.

5. The hoop stress for fracture depends on the machined radius of curvature of the crack tip, r, but it is suggested that the actual radius of curvature of the propagating crack, r_0, is much smaller.

References

1. W. BONFIELD and C. H. LI, *J. Appl. Phys.* **37** (1966) 869.
2. P. E. REED and H. D. SQUIRES, *J. Mater. Sci.* **9** (1974) 129.
3. E. H. ANDREWS, L. BERNSTEIN, P. J. NURSE and P. E. REED, in "Shock Tube Research", edited by J. Stollery (Chapman and Hall, London, 1971).
4. W. BONFIELD and E. A. CLARK, *J. Mater. Sci.* **8** (1973) 1590.
5. A. W. SWEENEY, R. K. BYERS and R. P. KROON, *Amer. Soc. Mech. Eng.* Publication 65-WA/HUF-7 (1965) p. 1.
6. J. H. MCELHANEY, *J. Appl. Physiol.* **21** (1966) 1231.
7. W. T. DEMPSTER and R. T. LIDDICOAT, *Amer. J. Anat.* **91** (1952) 331.
8. W. BONFIELD and P. K. DATTA, *J. Biomechanics*, **7** (1974) 147.
9. *Idem*, to be published.
10. E. H. ANDREWS, "Polymer Science", edited by A. D. Jenkins (North Holland, Amsterdam, 1972) p. 579.
11. A. A. GRIFFITH, *Phil. Trans. Roy. Soc. (London)* **A221** (1920) 163.

Received 22 March and accepted 3 April 1974.